

Intermolecular interactions in aniline/benzene hetero-trimer and aniline homo-trimer ions

Kazuhiko Ohashi^{a,*}, Yoshiya Inokuchi^b, Nobuyuki Nishi^b, Hiroshi Sekiya^a

^a *Department of Chemistry, Faculty of Sciences, Kyushu University,
Hakozaki, Fukuoka 812-8581, Japan*

^b *Institute for Molecular Science, Myodaiji, Okazaki 444-8585, Japan*

Received 14 February 2002

Abstract

The charge distribution and binding features of aniline/benzene hetero-trimer and aniline homo-trimer ions are investigated by vibrational spectroscopy and by near-infrared photodissociation and spontaneous unimolecular dissociation of mass-selected cluster ions. The absence of the charge resonance absorption indicates the charge localization in the trimer ions. Substantial red-shifts and enhanced intensities of the vibrational transitions suggest strong perturbations to the NH oscillators. The trimer ions are stabilized by the hydrogen-bonding interaction through the NH₂ group of the charged aniline with the neutral molecules rather than the charge-delocalization interaction among the component molecules.

* Corresponding author. Fax: +81-92-642-2607; e-mail: kazu.scc@mbox.nc.kyushu-u.ac.jp

1. Introduction

One of the central aims for studying clusters is elucidating their structures and understanding intermolecular interactions. Mass spectrometry is useful in determining gross structural and binding features of cluster ions through the observation of spontaneous unimolecular dissociation processes [1,2]. The least tightly bound molecule in a cluster ion is preferentially lost in the final stage of energy dissipation, if the process is controlled by energetics. Spectroscopic methods offer the most direct approach to structural investigations of cluster ions [3]. Vibrational spectroscopy is particularly suited for probing intermolecular interactions [4,5], because certain vibrational modes are quite sensitive to intermolecular perturbations. Electronic spectroscopy in the near-infrared wavelength region can be used to explore charge resonance (CR) interaction in cluster ions [6,7].

Previously, we studied intermolecular interactions in (aniline–benzene)⁺ and (aniline)₂⁺ using the electronic and vibrational spectroscopy [8]. The absence of the CR absorption indicates that the positive charge is localized on one component molecule in both systems. The vibrational spectrum of (aniline–benzene)⁺ suggests an NH– π -type hydrogen bond between the charged aniline and the neutral benzene. For (aniline)₂⁺, an NH bond of the charged aniline forms different types of hydrogen bond with the neutral aniline: one with the π -electrons of the aromatic ring (NH– π -type structure) and the other with the lone pair of the nitrogen atom (NH–N-type structure). Density functional theory calculations reveal that the NH–N-type structure is more stable than the NH– π -type structure [9]. The accretion of an additional molecule to these dimer ions possibly induces a change in the intermolecular interaction. For instance, (aniline–benzene–benzene)⁺ may be stabilized by the CR interaction in the benzene dimer subunit rather than the hydrogen-bonding interaction in the aniline–benzene subunit as in the case of (aniline–benzene)⁺.

The main purpose of this work is to characterize intermolecular interactions in the heterogeneous trimer ions composed of aniline (An) and benzene (Bz). Unimolecular dissociation pathways are investigated to determine the most weakly bound molecule in the trimer ions. Photodissociation behavior in the near-infrared region is examined for exploring

the CR interaction among the component molecules. Vibrational spectra in the NH-stretching region are recorded to obtain information on the hydrogen-bonding interaction.

2. Experimental

We perform three different experiments on the mass-selected trimer ions in the gas phase. The first experiment concerns the spontaneous unimolecular dissociation process. We use a time-of-flight (TOF) mass spectrometer with an ion reflector [10]. The trimer ions are produced from non-selective 2-photon ionization of larger clusters followed by instantaneous evaporation processes occurring in the spot of the ionization laser. TOF spectra are recorded for the fragment ions produced via the unimolecular dissociation of the trimer ions while traveling in the field-free region of the mass spectrometer. In the second experiment, the trimer ions are irradiated by a near-infrared laser while traveling in the acceleration region of the TOF mass spectrometer. The photodissociation cross sections are estimated from the intensity of the parent ions obtained with and without the laser. The third experiment is aimed at measuring the vibrational spectra of the trimer ions. We employ the infrared photodissociation spectroscopy using a triple quadrupole mass spectrometer [11]. Electron-impact ionization of a molecule in a jet expansion close to a nozzle orifice is followed by three-body association reactions with neutral molecules to form the trimer ions. The photodissociation spectra are taken by recording the yields of the fragment ions resulting from the vibrational predissociation of the trimer ions as a function of wavenumber of an infrared laser.

3. Results and discussion

3.1. Spontaneous unimolecular dissociation

The main dissociation pathway is known to be the evaporation of a single molecule in the unimolecular dissociation of molecular cluster ions on the 10–100 μ s time scale. The dissociation of benzene/toluene, benzene/cyclohexane and benzene/para-difluorobenzene hetero-cluster ions was investigated by Neusser and co-workers [1,2]. They found that the ejection of the most labile molecule is the dominant dissociation channel in the hetero-cluster ions.

Fig. 1a shows the TOF spectrum of the trimer ions. Ion signals labeled c–f are due to $(\text{Bz}\bullet\text{Bz}\bullet\text{Bz})^+$, $(\text{Bz}\bullet\text{Bz}\bullet\text{An})^+$, $(\text{Bz}\bullet\text{An}\bullet\text{An})^+$ and $(\text{An}\bullet\text{An}\bullet\text{An})^+$, respectively. Fig. 1b exhibits the spectrum of the fragment ions produced by the spontaneous dissociation of the trimer ions in the field-free region of the mass spectrometer. For measuring spectrum b, the field strength of the ion reflector is reduced to 2/3 of that for spectrum a; the reduction forces the fragment ions to follow the same flight path as the parent ions [12,13]. As a result, the flight times of $(\text{Bz}\bullet\text{Bz})^+$ (peak g) and $(\text{An}\bullet\text{An})^+$ (peak l) are the same as those of their parent ions $(\text{Bz}\bullet\text{Bz}\bullet\text{Bz})^+$ (peak c) and $(\text{An}\bullet\text{An}\bullet\text{An})^+$ (peak f), respectively. However, the ratio of masses of the fragment and parent ions is not exactly equal to 2/3 for the hetero-trimer ions. Thus we perform numerical calculations for simulating the flight times of the fragment ions to assign the other peaks seen in spectrum b. Only $(\text{Bz}\bullet\text{An})^+$ (peak i) turns out to be the fragment ion arising from $(\text{Bz}\bullet\text{Bz}\bullet\text{An})^+$; no signal is observed at the flight time expected for $(\text{Bz}\bullet\text{Bz})^+$ (position h). On the other hand, both $(\text{Bz}\bullet\text{An})^+$ (peak j) and $(\text{An}\bullet\text{An})^+$ (peak k) are detected as the products of $(\text{Bz}\bullet\text{An}\bullet\text{An})^+$, although the relative intensity of $(\text{Bz}\bullet\text{An})^+$ is considerably small. The neutral benzene molecule is preferentially lost from $(\text{Bz}\bullet\text{Bz}\bullet\text{An})^+$ and $(\text{Bz}\bullet\text{An}\bullet\text{An})^+$, indicating that it is the most labile species in the hetero-trimer ions.

3.2. Photodissociation in the near-infrared region

The electronic spectrum of $(\text{Bz}\bullet\text{Bz})^+$ shows intense CR bands in the near-infrared region [14]. The charge-delocalization interaction between the component molecules is responsible for the CR transitions. The CR bands characteristic of $(\text{Bz}\bullet\text{Bz})^+$ remain essentially intact in $(\text{Bz}\bullet\text{Bz}\bullet\text{Bz})^+$, indicating that the positive charge is carried by a dimer subunit in the trimer ion [11,15]. The dimer subunit acts as a chromophore for the strong near-infrared absorption in $(\text{Bz}\bullet\text{Bz}\bullet\text{Bz})^+$. In the present work, photodissociation cross sections of $(\text{Bz}\bullet\text{Bz}\bullet\text{An})^+$, $(\text{Bz}\bullet\text{An}\bullet\text{An})^+$ and $(\text{An}\bullet\text{An}\bullet\text{An})^+$ in the near-infrared region are compared with that of $(\text{Bz}\bullet\text{Bz}\bullet\text{Bz})^+$ for probing the CR interaction in these trimer ions.

Fig. 2a displays the TOF spectrum of the trimer ions without the photodissociation laser. Ion signals labeled c–f are due to $(\text{Bz}\bullet\text{Bz}\bullet\text{Bz})^+$, $(\text{Bz}\bullet\text{Bz}\bullet\text{An})^+$, $(\text{Bz}\bullet\text{An}\bullet\text{An})^+$ and $(\text{An}\bullet\text{An}\bullet\text{An})^+$, respectively. The introduction of the photodissociation laser at 950 nm results in the spectrum

given in Fig. 2b, where the packets of all the trimer ions are irradiated simultaneously. Approximately 50 % of the $(\text{Bz}\bullet\text{Bz}\bullet\text{Bz})^+$ signal is depleted by the laser, whereas the depletion is not seen in the signals of the other ions. The experiment with the photodissociation laser at 1200 nm yields essentially the same result. The absence of the depletion in the ion signals indicates that the photodissociation cross sections of $(\text{Bz}\bullet\text{Bz}\bullet\text{An})^+$, $(\text{Bz}\bullet\text{An}\bullet\text{An})^+$ and $(\text{An}\bullet\text{An}\bullet\text{An})^+$ are negligibly small at these wavelengths. The CR interaction is insignificant in these trimer ions; the dominant contribution to the binding energy is probably from the hydrogen-bonding interaction rather than the CR interaction.

3.3. Vibrational spectra

Fig. 3 exhibits the vibrational predissociation spectra of (a) $(\text{Bz}\bullet\text{Bz}\bullet\text{Bz})^+$, (b) $(\text{An}\bullet\text{An}\bullet\text{An})^+$, (c) $(\text{Bz}\bullet\text{An}\bullet\text{An})^+$, (d) $(\text{Bz}\bullet\text{Bz}\bullet\text{An})^+$ and (e) $(\text{Bz}\bullet\text{An})^+$. The spectra of $(\text{Bz}\bullet\text{Bz}\bullet\text{Bz})^+$ [11] and $(\text{Bz}\bullet\text{An})^+$ [8] have been already published and are included here for reference. A sharp transition centered at 3066 cm^{-1} in the spectrum of $(\text{Bz}\bullet\text{Bz}\bullet\text{Bz})^+$ originates from a CH-stretching vibration. Weak features seen in the $3000\text{--}3100\text{-cm}^{-1}$ region of spectra b–e are possibly assigned to the CH-stretching vibrations. Most of the prominent bands observed in the $3100\text{--}3500\text{-cm}^{-1}$ region can be attributed to the NH-stretching vibrations of the charged aniline, because the infrared absorption intensity of the charged moiety is much larger than that of the neutral moiety in $(\text{An}\bullet\text{An})^+$ [9,16]. Nakanaga et al. observed the symmetric and antisymmetric NH stretching vibrations of $\text{An}^+\bullet\text{Ar}$ at 3394.5 and 3488.0 cm^{-1} , respectively [17]. These frequencies of $\text{An}^+\bullet\text{Ar}$ are considered to be essentially the same as those of the bare An^+ , because the NH_2 group of An^+ is hardly perturbed by the argon atom on the aromatic ring. If hydrogen bonds are formed through the NH_2 group, we can expect a large red-shift and a substantial broadening of the bands due to the NH stretching vibrations. Three distinct transitions are seen around 3200 , 3280 and 3330 cm^{-1} in the spectrum of $(\text{Bz}\bullet\text{Bz}\bullet\text{An})^+$. The spectrum of $(\text{Bz}\bullet\text{An}\bullet\text{An})^+$ displays a prominent band centered at 3300 cm^{-1} and weak features around 3200 and 3420 cm^{-1} ; the former band can be deconvoluted into three transitions at 3280 , 3300 and 3340 cm^{-1} . For $(\text{An}\bullet\text{An}\bullet\text{An})^+$, two maxima are seen near 3280 and 3420 cm^{-1} with an underlying broad feature extending from 3000 to 3500 cm^{-1} .

A brief review of the previous study of $(\text{Bz}\bullet\text{An})^+$ is helpful in assigning the spectra of the trimer ions. The structure of $(\text{Bz}\bullet\text{An})^+$ involves an NH- π -type hydrogen bond between one of the NH bonds of the ionic aniline and the π -electrons of the neutral benzene [8]. The 3200- cm^{-1} band of $(\text{Bz}\bullet\text{An})^+$ is attributed to the stretching vibration of the hydrogen-bonded NH oscillator. The 3440- cm^{-1} band is assigned to the NH oscillator free from the hydrogen bond. We tentatively attribute the transition at 3280 cm^{-1} to the overtone of the NH_2 -bending vibration or the overtone of the ring-stretching vibration after the assignment proposed by Schmid et al. [18]. Recently, Solcà and Dopfer have observed the corresponding band in the infrared spectra of $\text{An}^+\bullet(\text{N}_2)_n$ [19]. They ascribe the band to the overtone of the NH_2 -bending vibration on the basis of the frequency shift as a function of n .

3.4. Charge distribution in the trimer ions

As described in section 3.2, the charge-delocalization interaction is insignificant in the trimer ions with aniline. In such a situation, the positive charge is prone to reside on a subunit with the lowest ionization energy (IE). Among subunits in $(\text{Bz}\bullet\text{Bz}\bullet\text{An})^+$, the IE values of $\text{Bz}\bullet\text{Bz}$ and An are reported to be 8.65 [1,20] and 7.7206 eV [21], respectively. The IE value of the $\text{Bz}\bullet\text{An}$ subunit may be smaller than these values, but the charge is shown to be localized on An even in $(\text{Bz}\bullet\text{An})^+$ [8]. Consequently, the charge carrier in $(\text{Bz}\bullet\text{Bz}\bullet\text{An})^+$ is expected to be the aniline molecule. For $(\text{Bz}\bullet\text{An}\bullet\text{An})^+$, the $\text{An}\bullet\text{An}$ subunit probably has the smallest IE value, but the charge resides on one An even in $(\text{An}\bullet\text{An})^+$ [8]. Similarly, the charge is considered to be carried by one An molecule in $(\text{An}\bullet\text{An}\bullet\text{An})^+$. For all the trimer ions that include at least one An molecule, the positive charge is localized on a single An molecule. The charge localization on a single component molecule is also demonstrated for $(\text{phenol})_n^+$ with $n = 2-4$ [6,22].

3.5. Structure of the trimer ions

The transition due to the hydrogen-bonded NH oscillator of $(\text{Bz}\bullet\text{An})^+$ remains intact at 3200 cm^{-1} in the spectrum of $(\text{Bz}\bullet\text{Bz}\bullet\text{An})^+$ (Fig. 3). On the other hand, there is a new band centered near 3330 cm^{-1} , replacing the 3440- cm^{-1} band of $(\text{Bz}\bullet\text{An})^+$ due to the free NH

oscillator. The 3330-cm⁻¹ band is as strong as the 3200-cm⁻¹ band. These facts suggest that each NH oscillator in (Bz•Bz•An)⁺ is subject to a large perturbation as a result of the formation of the hydrogen bond with a benzene molecule. Fig. 4a shows a schematic illustration of the structure proposed for (Bz•Bz•An)⁺. We assign the transitions at 3200 and 3330 cm⁻¹ to the symmetric and antisymmetric stretching vibrations of the hydrogen-bonded NH₂ group, respectively. The 3280-cm⁻¹ band can be interpreted as the overtone of the NH₂-bending vibration. The hydrogen-bonded structure of the NH-π/NH-π-type is consistent with the observation of only (Bz•An)⁺ as the product of the unimolecular dissociation, because the production of (Bz•Bz)⁺ requires the cleavage of the two hydrogen bonds.

The positive charge is localized on one of the two aniline molecules in (Bz•An•An)⁺. The charged aniline molecule acts as a proton donor in hydrogen bonds, because the acidity of the charged aniline is stronger than that of the neutral aniline [18]. One NH bond of the charged aniline is expected to form an NH-π-type hydrogen bond with benzene. The other NH bond is able to form two types of hydrogen bond with the neutral aniline: one with the lone pair of the nitrogen atom and the other with the π-electrons of the aromatic ring. The resulting structures of (Bz•An•An)⁺ are schematically illustrated in Figs. 4b and 4c. The structure involving an NH-N-type hydrogen bond (Fig. 4b) is expected to be more stable than the other one involving an NH-π-type hydrogen bond (Fig. 4c), because the former bond is stronger than the latter one, as confirmed in the previous study of (An•An)⁺ [8,9]. The expectation is supported by the vibrational spectrum of (Bz•An•An)⁺. The band centered at 3300 cm⁻¹ is assigned to the stretching vibration of the NH oscillator forming the NH-π-type hydrogen bond with benzene. As in the case of (An•An)⁺, the absorption of the NH oscillator hydrogen-bonded to the nitrogen atom of the neutral aniline probably shifts to an extremely low frequency and becomes substantially broad, so that it is not seen as a distinct band in the spectrum. The absorption at 3280 cm⁻¹ can be attributed to the overtone of the NH₂-bending vibration. The features around 3340 and 3420 cm⁻¹ possibly represent the symmetric and antisymmetric stretching vibrations of the NH₂ group, respectively, of the proton-accepting aniline of a neutral character. As a consequence of the unimolecular dissociation of the NH-π/NH-N-type structure (Fig. 4b), the intensity of (An•An)⁺ becomes larger than that of (Bz•An)⁺, because the

NH- π -type hydrogen bond between An⁺ and Bz is broken more likely than the NH-N-type hydrogen bond between An⁺ and An. The slight absorption near 3200 cm⁻¹ suggests the presence of the NH- π /NH- π -type structure (Fig. 4c) as a minor isomer, because the position coincides with the 3200-cm⁻¹ band of (Bz•Bz•An)⁺.

After considering the structure of (Bz•An•An)⁺, it seems natural to expect that each NH bond of An⁺ is bound to the nitrogen atom of An in the most stable structure of (An•An•An)⁺. The NH-N/NH-N-type structure depicted in Fig. 4d is fairly consistent with the vibrational spectrum of (An•An•An)⁺. The stretching vibrations of the hydrogen-bonded NH₂ of the charged aniline are probably responsible for the broad feature in the 3000–3500 cm⁻¹ region, which are not observed as distinct bands because of large red-shifts and substantial broadening. The remaining maximum around 3280 cm⁻¹ is attributable to the overtone of the NH₂-bending vibration. The weaker features around 3330 and 3420 cm⁻¹ may be due to the NH₂ group of the neutral An molecule. As can be seen from Fig. 4d, an NH- π -type hydrogen bond is possible between the neutral An molecules. The additional hydrogen bond may be responsible for the anomalous stability of (An•An•An)⁺ observed as a magic number in the mass spectrum of (An)_n⁺ [23]. Theoretical calculations at reliably high levels are desired for discussing the structure of the trimer ions in further detail.

4. Conclusions

We have investigated the gross structural and binding features of (Bz•Bz•An)⁺, (Bz•An•An)⁺ and (An•An•An)⁺ by the vibrational spectroscopy of the NH-stretching modes and by the near-infrared photodissociation and the spontaneous unimolecular dissociation of mass-selected cluster ions. The observed pathways for the unimolecular dissociation of (Bz•Bz•An)⁺ and (Bz•An•An)⁺ demonstrate that Bz is the most weakly bound molecule in the hetero-trimer ions. The negligibly small photodissociation cross sections in the near-infrared region indicate that the positive charge is localized on a single An molecule in all the trimer ions. The vibrational spectrum suggests the NH- π /NH- π -type hydrogen-bonded structure for (Bz•Bz•An)⁺, where each NH bond of An⁺ is attached to the π -electrons of Bz. The NH- π /NH-N-type structure turns out to be the dominant isomer of (Bz•An•An)⁺, where one

NH bond of An^+ is bound to the π -electrons of Bz and the other to the nitrogen atom of An. The spectral features of $(An\bullet An\bullet An)^+$ are fairly consistent with the NH–N/NH–N-type structure. The trimer ions are stabilized by the hydrogen-bonding interaction through the NH_2 group of An^+ rather than the charge-delocalization interaction among the component molecules.

Acknowledgements

This work was supported in part by the Joint Studies Program (2001) of the Institute for Molecular Science and the Grant-in-Aid for Scientific Research (No. 11440177) from the Ministry of Education, Culture, Sports, Science and Technology of Japan.

References

- [1] B. Ernstberger, H. Krause, A. Kiermeier, H. J. Neusser, *J. Chem. Phys.* 92 (1990) 5285.
- [2] H. Krause, B. Ernstberger, J. J. BelBruno, H. J. Neusser, *J. Chem. Phys.* 95 (1991) 3302.
- [3] E. J. Bieske, J. P. Maier, *Chem. Rev.* 93 (1993) 2603.
- [4] J. M. Lisy, in: C. Y. Ng, T. Baer, I. Powis (Eds.), *Cluster Ions*, John Wiley & Sons, Chichester, 1993, p. 217.
- [5] M. W. Crofton, J. M. Price, Y. T. Lee, in: H. Haberland (Ed.), *Clusters of Atoms and Molecules II*, Springer, Berlin, 1994, p. 44.
- [6] K. Ohashi, Y. Inokuchi, N. Nishi, *Chem. Phys. Lett.* 257 (1996) 137.
- [7] K. Ohashi, H. Izutsu, Y. Inokuchi, K. Hino, N. Nishi, H. Sekiya, *Chem. Phys. Lett.* 321 (2000) 406.
- [8] K. Ohashi, Y. Inokuchi, H. Izutsu, K. Hino, N. Yamamoto, N. Nishi, H. Sekiya, *Chem. Phys. Lett.* 323 (2000) 43.
- [9] N. Yamamoto, K. Ohashi, K. Hino, H. Izutsu, K. Mogi, Y. Sakai, H. Sekiya, *Chem. Phys. Lett.* 345 (2001) 532.
- [10] K. Ohashi, N. Nishi, *J. Chem. Phys.* 95 (1991) 4002.
- [11] Y. Inokuchi, N. Nishi, *J. Chem. Phys.* 114 (2001) 7059.
- [12] S. Wei, W. B. Tzeng, A. W. Castleman, Jr., *J. Chem. Phys.* 92 (1990) 332.
- [13] S. Wei, W. B. Tzeng, A. W. Castleman, Jr., *J. Chem. Phys.* 93 (1990) 2506.
- [14] K. Ohashi, Y. Nakai, T. Shibata, N. Nishi, *Laser Chem.* 14 (1994) 3.
- [15] K. Ohashi, N. Nishi, *J. Chem. Phys.* 109 (1998) 3971.
- [16] T. Nakanaga, P. K. Chowdhury, F. Ito, K. Sugawara, H. Takeo, *J. Mol. Struct.* 413–414 (1997) 205.

- [17] T. Nakanaga, F. Ito, J. Miyawaki, K. Sugawara, H. Takeo, *Chem. Phys. Lett.* 261 (1996) 414.
- [18] R. P. Schmid, P. K. Chowdhury, J. Miyawaki, F. Ito, K. Sugawara, T. Nakanaga, H. Takeo, H. Jones, *Chem. Phys.* 218 (1997) 291.
- [19] N. Solcà, O. Dopfer, in preparation.
- [20] A. Kiermeier, B. Ernstberger, H. J. Neusser, E. W. Schlag, *J. Phys. Chem.* 92 (1988) 3785.
- [21] X. Song, M. Yang, E. R. Davidson, J. P. Reilly, *J. Chem. Phys.* 99 (1993) 3224.
- [22] A. Fujii, A. Iwasaki, K. Yoshida, T. Ebata, N. Mikami, *J. Phys. Chem. A* 101 (1997) 1798.
- [23] K. Ohashi, Y. Inokuchi, N. Nishi, H. Sekiya, in preparation.

Figure Captions

Fig. 1. (a) TOF spectrum of the parent trimer ions. c: $(\text{Bz}\bullet\text{Bz}\bullet\text{Bz})^+$; d: $(\text{Bz}\bullet\text{Bz}\bullet\text{An})^+$; e: $(\text{Bz}\bullet\text{An}\bullet\text{An})^+$; f: $(\text{An}\bullet\text{An}\bullet\text{An})^+$. (b) TOF spectrum of the fragment dimer ions produced by unimolecular dissociation of the trimer ions in the field-free region of the mass spectrometer. The sensitivity of the detection system is increased by a factor of 10 and the field strength of the ion reflector is reduced to 2/3 of that for spectrum a. Ion signals labeled g–l are assigned as follows. g: $(\text{Bz}\bullet\text{Bz})^+$ from $(\text{Bz}\bullet\text{Bz}\bullet\text{Bz})^+$; h: flight time expected for $(\text{Bz}\bullet\text{Bz})^+$ from $(\text{Bz}\bullet\text{Bz}\bullet\text{An})^+$; i: $(\text{Bz}\bullet\text{An})^+$ from $(\text{Bz}\bullet\text{Bz}\bullet\text{An})^+$; j: $(\text{Bz}\bullet\text{An})^+$ from $(\text{Bz}\bullet\text{An}\bullet\text{An})^+$; k: $(\text{An}\bullet\text{An})^+$ from $(\text{Bz}\bullet\text{An}\bullet\text{An})^+$; l: $(\text{An}\bullet\text{An})^+$ from $(\text{An}\bullet\text{An}\bullet\text{An})^+$.

Fig. 2. (a) TOF spectrum of the trimer ions. c: $(\text{Bz}\bullet\text{Bz}\bullet\text{Bz})^+$; d: $(\text{Bz}\bullet\text{Bz}\bullet\text{An})^+$; e: $(\text{Bz}\bullet\text{An}\bullet\text{An})^+$; f: $(\text{An}\bullet\text{An}\bullet\text{An})^+$. There are differences in the flight times and relative intensities of the trimer ions between Figs 1a and 2a, because the two measurements are performed under different experimental conditions. (b) TOF spectrum obtained with the introduction of the photodissociation laser at 950 nm, where the packets of all the trimer ions are irradiated simultaneously. It should be noted that the absence of the depletion in the signals of $(\text{Bz}\bullet\text{Bz}\bullet\text{An})^+$, $(\text{Bz}\bullet\text{An}\bullet\text{An})^+$ and $(\text{An}\bullet\text{An}\bullet\text{An})^+$ is not due to an incomplete overlap of the ion packets with the laser beam.

Fig. 3. Vibrational spectra of (a) $(\text{Bz}\bullet\text{Bz}\bullet\text{Bz})^+$ [11], (b) $(\text{An}\bullet\text{An}\bullet\text{An})^+$, (c) $(\text{Bz}\bullet\text{An}\bullet\text{An})^+$, (d) $(\text{Bz}\bullet\text{Bz}\bullet\text{An})^+$ and (e) $(\text{Bz}\bullet\text{An})^+$ [8] obtained by monitoring the yields of (a) $(\text{Bz}\bullet\text{Bz})^+$, (b) $(\text{An}\bullet\text{An})^+$, (c) $(\text{An}\bullet\text{An})^+$, (d) $(\text{Bz}\bullet\text{An})^+$ and (e) An^+ as a function of wavenumber of the laser.

Fig. 4. Schematic illustration of hydrogen-bonded structures of the trimer ions. (a) $(\text{Bz}\bullet\text{Bz}\bullet\text{An})^+$ (NH– π /NH– π -type), (b) $(\text{Bz}\bullet\text{An}\bullet\text{An})^+$ (NH– π /NH–N-type), (c) $(\text{Bz}\bullet\text{An}\bullet\text{An})^+$ (NH– π /NH– π -type) and (d) $(\text{An}\bullet\text{An}\bullet\text{An})^+$ (NH–N/NH–N-type). Mutual orientation of pairs of a proton-donor and a proton-acceptor in structures a–c is drawn on the basis of the theoretical calculations for $(\text{Bz}\bullet\text{An})^+$ and $(\text{An}\bullet\text{An})^+$ [9].

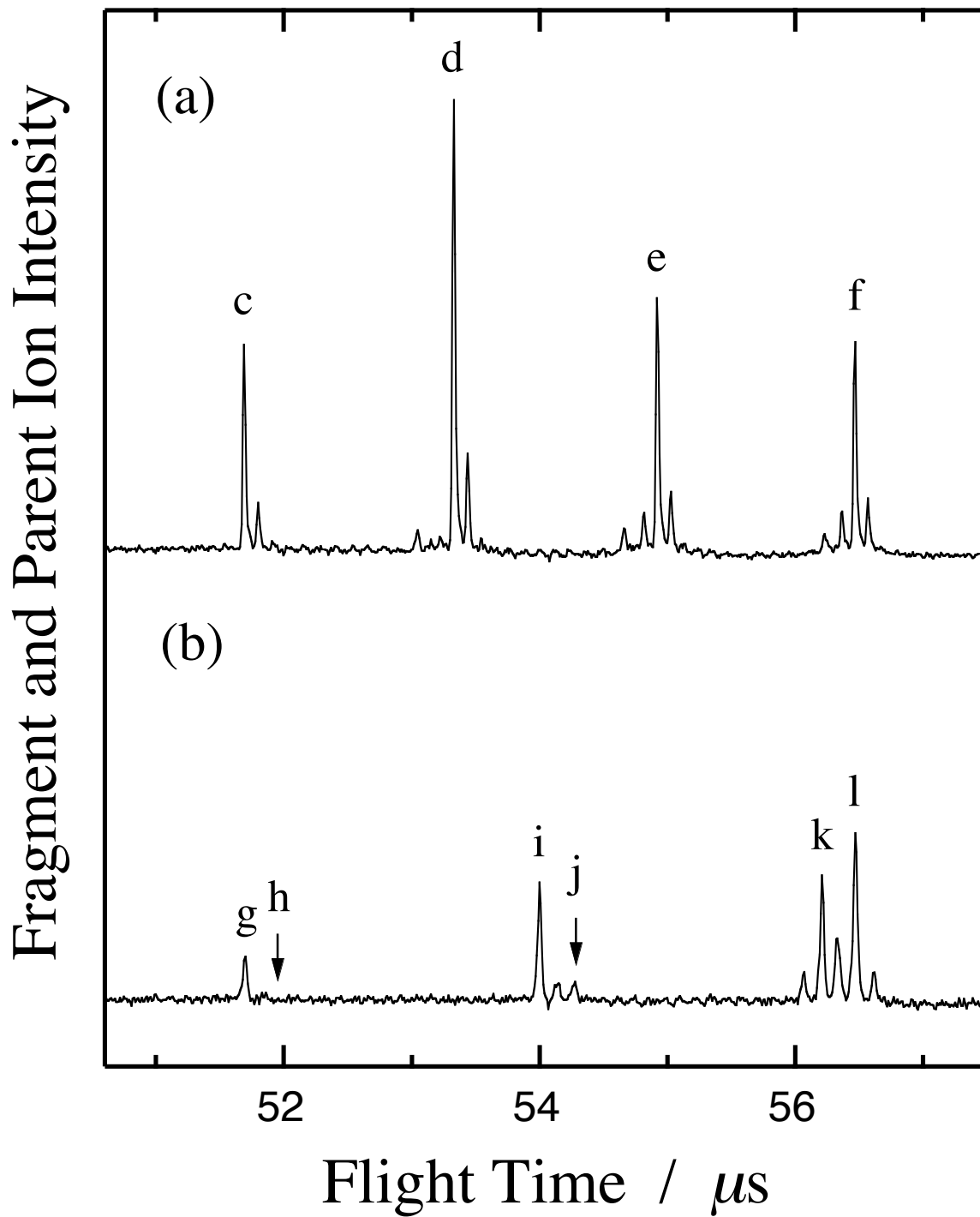


Fig. 1. Ohashi et al.

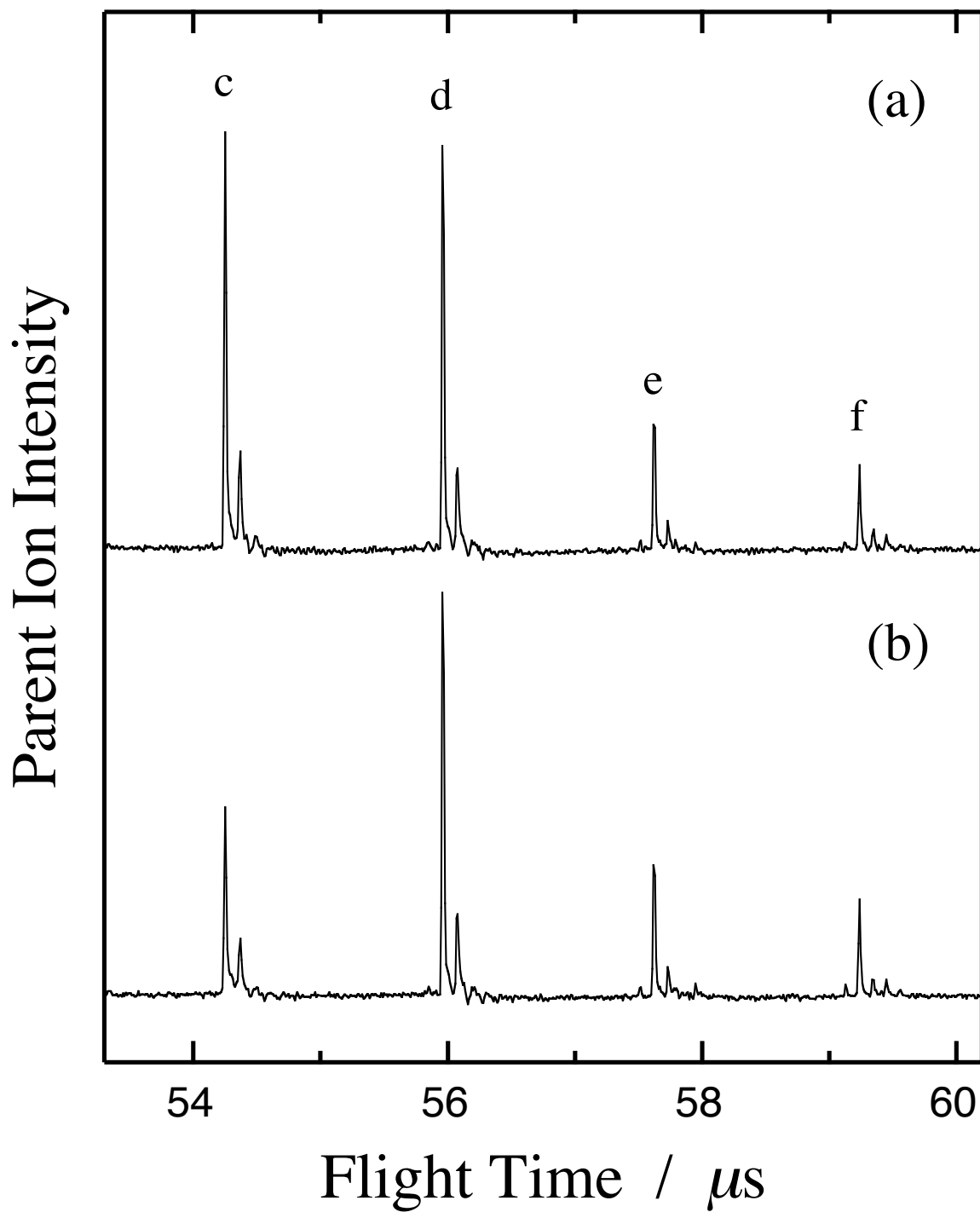


Fig. 2. Ohashi et al.

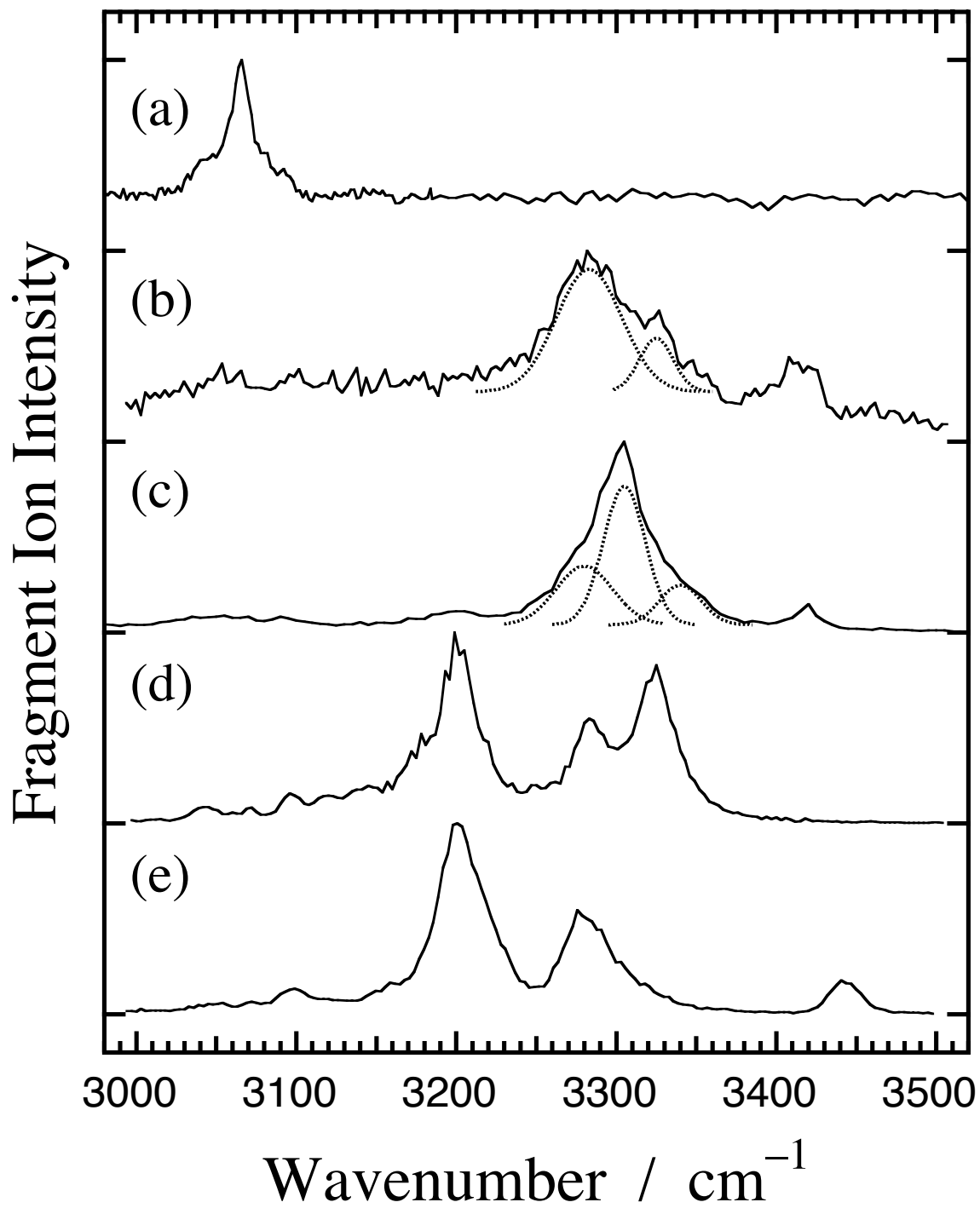


Fig. 3. Ohashi et al.

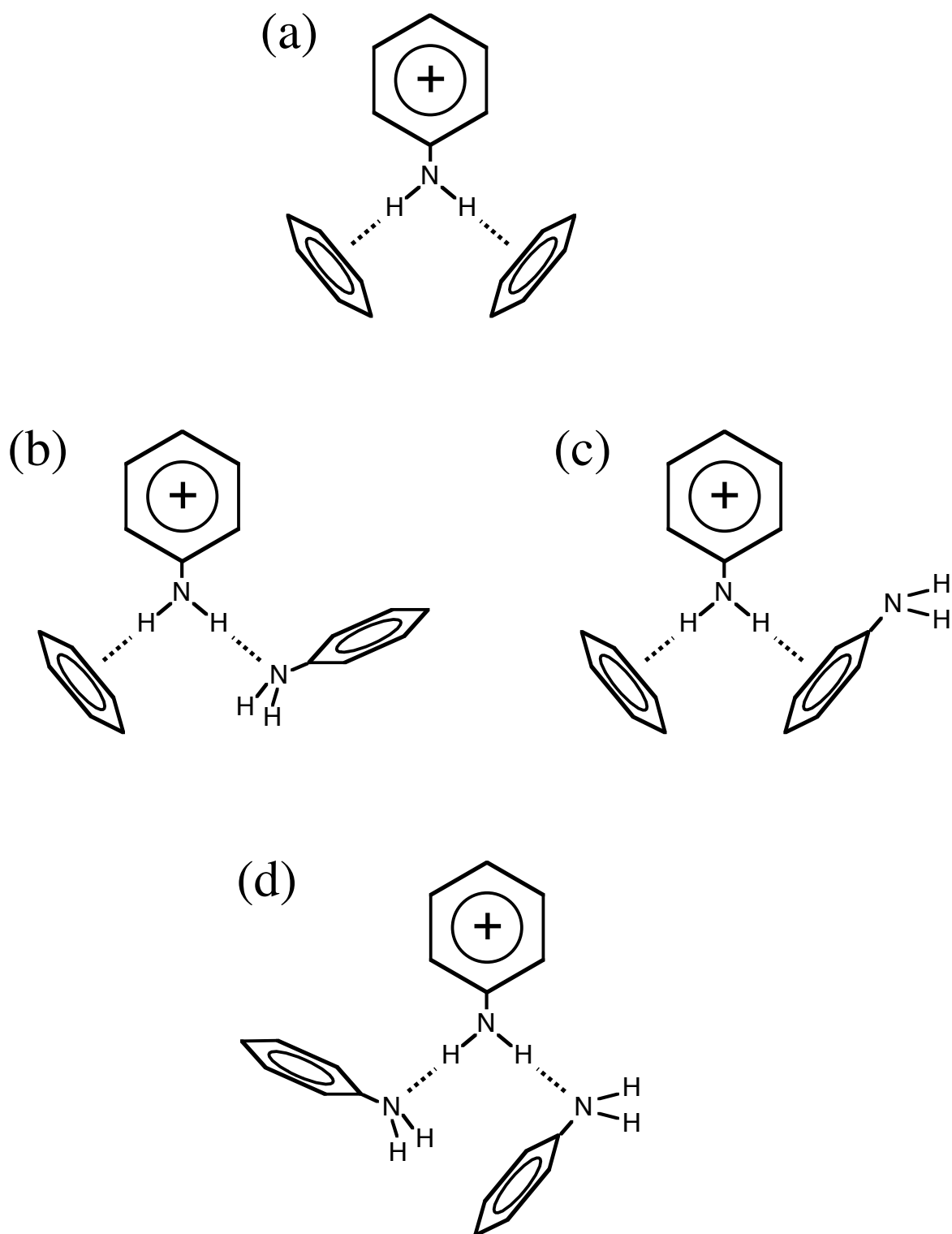


Fig. 4. Ohashi et al.